Journal of the European Ceramic Society 41 (2021) 7792–7806

Contents lists available at ScienceDirect

Journal of the European Ceramic Society

journal homepage: www.elsevier.com/locate/jeurceramsoc

Corrosion resistant ZrO_2/SiC ultrafiltration membranes for wastewater treatment and operation in harsh environments

Fabrício Eduardo Bortot Coelho [a], Nicolaj N. Kaiser [c], Giuliana Magnacca [a,b], Victor M. Candelario [c,*]

[a] Department of Chemistry, University of Turin, Via P. Giuria 7, 10125, Turin, Italy
[b] NIS Interdepartmental Centre, University of Turin, Via P. Giuria 7, 10125, Turin, Italy
[c] Liqtech Ceramics A/S, Industriparken 22 C, 2750, Ballerup, Denmark

ARTICLE INFO

Keywords:
Zirconia
Silicon carbide
Wastewater treatment
Oil separation
Corrosion resistance

ABSTRACT

This work focused on the fabrication of a ZrO_2/SiC ultrafiltration membrane by dip coating a high porous SiC support with a ZrO_2 slurry prepared by ceramic processing. The membranes were sintered in different temperatures (1000−1300 °C). With the optimal temperature, it was obtained a mechanically strong, homogenous, and defect free separation layer with 45 μm of thickness and average pore size of 60 nm. A pure water permeability of 360 $L.m^{-2}\ h^{-1}\ bar^{-1}$ and high retentions of humic acid, indigo dye, and hemoglobin were observed. In a pilot test with an olive oil/water emulsion, 99.91 % of oil was removed without fouling. Long-term corrosion tests at basic and acid baths did not cause change in pore size and morphology. In conclusion, the ZrO_2/SiC membrane has potential to operate in harsh conditions (*e.g.* heavily contaminated industrial effluents or urban wastewaters) and when severe membrane cleaning and disinfection are required, such as food and pharmaceutical industries.

1. Introduction

Ceramic membranes present excellent mechanical, chemical and thermal properties compared to traditional polymeric membranes [1], which allows them to operate in a wide range of pH and elevated temperatures. On the other hand, the fabrication of these membranes may be complex and involve high manufacture costs [2]. Nevertheless, ceramic membranes can be backwashed and regenerated under more harsh cleaning conditions, resulting in a longer lifetime [3,4]. Furthermore, these membranes are resistant to organic solvents and provide higher fluxes than polymeric membranes owing to their mechanical stability under elevated pressure gradients and high structural integrity [5]. Thermic resistant membranes are required in some specific filtration processes, such as in textile (up to 90 °C), sugar (70–80 °C), pulp and paper (> 60 °C) industries, since high temperatures offer various advantages in terms of increasing process efficiency, such as recovering heat from hot streams, and protection of plant installations [6–8]. Chemical resistance is required not only for proper cleaning but also for acid or basic feeds, such as in wastewater treatment [9], metallurgy industry, radioactive feeds [10], and aggressive solvents [11].

In this way, most of commercial ceramic membranes available are traditionally made of silica, zeolite, and alumina [12] own to these materials cost-effectiveness and easiness to tailor the membranes porosity [13] when compared to other materials such as silicon carbide, zirconia, and titania. Nevertheless, the practical application of these membranes has been limited, mainly because of the insufficient chemical and thermal stability of SiO_2 and Al_2O_3 under corrosive and aggressive conditions such as $3 > pH > 10$ and hydrothermal environments (300 °C, 15 bar) [14–16].

On the contrary, zirconia (ZrO_2) is a promising material for ceramic membranes owing to its several advantageous properties. ZrO_2 is a refractory material that can work at high temperatures [2], being applied for hot gases separations, membrane reactors, and solid-state fuel cells [14]. In addition, zirconia high chemical stability makes it suitable to work in conditions where silica and alumina membranes fail [9,17,18], especially in strong alkaline media [5]. This allows severe cleaning and disinfection of ZrO_2 membranes [19]. Furthermore, such zirconia membranes have high hydrophilicity [4,9], which leads to higher fluxes and lower fouling during water treatment [3]. Therefore, ZrO_2 membranes have been widely applied as top separation layer in MF, UF, and NF processes, that include wastewater treatment [9], aggressive solvents, high salinity, radioactive [10] or heavily contaminated feeds [11,

* Corresponding author.
E-mail address: vcl@liqtech.com (V.M. Candelario).

https://doi.org/10.1016/j.jeurceramsoc.2021.07.054
Received 28 June 2021; Received in revised form 21 July 2021; Accepted 26 July 2021
Available online 29 July 2021

20], hydrothermal conditions [14] and oil-water separation [21,22].

Although extensive studies have been performed on the preparation of zirconia membranes, most of them used alumina supports [20,21, 23–28], which do not have the required chemical and thermal stability, limiting their application [14]. A corrosion-resistant support could be obtained with silicon carbide (SiC), a great alternative to traditional materials [29–31], since it presents excellent chemical and thermal stabilities in extreme conditions, such as strong alkaline media or high temperature (600−800 °C) environments [32]. Furthermore, SiC shows low thermal expansion coefficient, high thermal conductivity, and super-hydrophilic properties with a water contact angle below 5 ° [33, 34], implying in lower fouling tendency and higher permeate fluxes in wastewater treatment [35]. Even though SiC emerged as an excellent porous support among the other ceramic materials [36–39], it is not suitable for UF applications, since pure silicon carbide membranes usually have pore sizes higher than 0.1 μm [32,40,41].

Concerning these aspects, an asymmetric composite membrane, in which a ZrO_2 UF selective layer is coated on a macroporous SiC substrate, should have the chemical resistance and the water permeability suitable for producing a high-performance membrane. However, few are the works devoted to the development of ZrO_2 membranes on SiC support [34,42] considering that there are several challenges in the ceramic processing (slurry) and sol-gel routes used in its fabrication. This process needs to overcome the following issues: to form a homogeneous thin layer of ZrO_2 by controlling the viscosity of the dipping fluid and its particle/sol size to avoid excessive infiltration into the support [18,43, 44]; and to avoid the cracks that can occur during the high temperature sintering because of ZrO_2 and SiC different thermal expansion coefficients [45] and the big volume variation that zirconia undergoes in the monoclinic/tetragonal phase transition [2,5].

Li et al. [42] reported a modified colloidal sol-gel method to obtain a ZrO_2 membrane on a self-made SiC support (average pore size 5.2 μm). Sintering the membranes at 700 and 900 °C, they obtained average pore sizes of 63 and 48 nm, respectively, with pure water permeability of 355 and 273 L m^{-2} h^{-1} bar^{-1}, respectively. Although the sol-gel method results in the formation of smooth and defect-free membranes, usually it requires expensive precursors, such as zirconium alkoxides, and organic solvents, which increase the cost and the environmental footprint [24, 46]. In addition, sol-gel processes involve several steps like hydrolysis and polymerization under controlled pH [46,47], which makes it more difficult for its industrial scale-up compared to ceramic processing. This process is significantly simpler than the sol-gel method and does not involve the use of metal alkoxides making it cost-effective. Ceramic processing allows obtaining uniform UF membrane layers with tailor-made pore size [23]. Li et al. [34] prepared a 3-YSZ (yttria-stabilized zirconia with 3 % molarY_2O_3) UF membrane by dip coating a SiC support (pore size of 1−2 μm) with a suspension of particles (average diameter 50 nm). In order to achieve that, the authors firstly coated the support with a SiC intermediate layer with a pore size of 0.9 μm. The membrane sintered at 800 °C for 45 min presented an average pore size of 82 nm with a water flux of 850 L m^{-2} h^{-1}. However, no filtration tests under real conditions were performed whereas the performance of developed membranes in their actual application setting needs to be tested to achieve a complete evaluation.

In this regard, considering chemically resistant membranes, it is quite relevant to evaluate their performance in wastewater treatments. Zirconia membranes have a particular application in the filtration of eluents containing oils, own to ZrO_2 especial surface properties such as high hydrophilicity [21,48]. These membranes have a superior performance in oil removal from oil in water emulsions, especially when chemical methods are ineffective, *i.e.* the oil droplets have a diameter less than 10−20 μm and are in a low concentration [48,49], separations higher than 99 % [49] can be achieved by filtration. Oily wastewaters are one of the major pollutants of the aquatic environment [49]. These hazardous effluents come from many industrial processes, such as petrochemical, tanning and leather industries, as well as cosmetics and food production [36]. In the Mediterranean countries, the annual olive oil production of 2.6 million tons [36] generates a huge volume of wastewaters that need to be treated before their discharge into the watercourses. Therefore, a pilot-scale filtration of an olive oil/water emulsion was carried out under real conditions, in order to evaluate the ZrO_2/SiC membrane separation performance, fouling behaviour and the possibility of water reuse.

In view of what it was exposed, the present paper focuses on the development and characterization of an ultrastable ultrafiltration zirconia membrane on tubular multi-channelled SiC supports. The ceramic processing was the technique applied for fabricating the monoclinic zirconia membrane, which was then characterized focusing on material properties and filtration aspects. A pilot-scale filtration test was carried out with a simulated wastewater containing olive oil to evaluate the performance of the new membrane in potential applications for oil removal.

2. Materials and methods

2.1. Powder characterization and dispersion studies

Two types of commercially available monoclinic zirconia (ZrO_2) powders with different particle sizes were selected to fabricate the membranes. According to the manufacturer (Imerys Fused Minerals, Germany), one powder has particle size below 1 μm (denoted as Z-1) while the other one below 2 μm (denoted as Z-2). They consist of fused zirconia (ZrO_2+HfO_2 ≥ 98.30 %wt) produced from zircon sand in an electric arc furnace at 2600 °C.

X-ray diffraction (XRD) patterns of the starting powders and sintered membranes were obtained with the diffractometer PW3040/60 X'Pert PRO MPD (Malvern Panalytical, Netherlands), operated at 45 kV and 40 mA with Cu-Kα radiation (λ = 1.5418 Å).

Nitrogen adsorption-desorption isotherms were obtained on a Micromeritics ASAP 2020 (Micromeritics, USA) equipment for the determination of surface area, using the Brunauer–Emmett–Teller (BET) model, and pore size distribution, using the Barrett-Joyner-Halenda (BJH) model applied to the adsorption branch of the isotherms. Before the adsorption run, all the samples were outgassed under vacuum (residual pressure 10^{-2} mbar) at 300 °C for 8 h to make surface and pores available for the subsequent N_2 adsorption.

Scanning electron microscopy (SEM) analyses were carried out by using a ZEISS EVO 50 XVP microscope with LaB_6 source, equipped with detectors for backscattered electrons, secondary electrons, and energy dispersive X-ray Spectroscopy (EDS). SEM micrographs were obtained after sputtering samples with a 10−15 nm thick gold film.

Since the ceramic processing was the technique applied to prepare the zirconia membranes, the first required condition was to obtain a stable suspension of the ZrO_2 powders in water. Then, in order to determine the influence of pH, dispersant concentration, and ball milling time on the suspension stability, several zeta potential and particle size analyses were performed. Particle size was determined by laser diffraction on a S3500 equipment (Microtrac Retsch GmbH, Germany). Dynamic Light Scattering (DLS) and Zeta potential measurements were performed on a Zetasizer Nano ZS (Malvern Instruments, United Kingdom). Briefly, powder suspensions (0.1 % w/v) were prepared in ultrapure water and ultrasonicated for 10 min before the analysis. The pH was adjusted with solutions of NaOH and HCl.

As dispersants, two commercial products were selected based on previous works on zirconia dispersions [50,51]. According to the manufacturers, Dolapix CE 64 (Zschimmer and Schwarz GmbH, Germany) is a carboxylic acid-based polyelectrolyte, free from alkali, with a molecular weight 320 Da, and an active matter of 65 % [52]. Duramax™ D-3005 (Dow, USA) is an ammonium salt of a polyacrylic acid with a molecular weight of 2400 Da and active matter of 35 %.

2.2. Membrane fabrication

The ZrO_2 membrane layer was coated on highly porous multi-channeled SiC tubular supports supplied by Liqtech Ceramics A/S (Denmark). Each support has 25 ± 1 mm of outer diameter, a total length of 305 ± 1 mm, and 30 cylindrical channels of 3 mm diameter each (Fig. 2a and b). Initial screening of processing parameters and harness characterization were conducted on flat sheet SiC supports with same pore characteristics of the tubular supports. Once optimized the ZrO_2 membrane layer preparation, tubular multi-channelled SiC supports were used for the coating.

The coating suspensions were a mixture of the fine (Z-1) and the coarse (Z-2) zirconia powders (in an equal mass ratio) dispersed in deionized water added with the dispersant and the binder. Solid contents between 10 and 30 wt% were investigated. The dispersant dosage was 2 wt% in relation to the mass of added powder. Temporary binders provided by Zschimmer and Schwarz GmbH (Germany), Optapix CS 76, a polysaccharide dicarbonic acid polymer, and Optapix PAF 2, a polyvinyl alcohol preparation, were investigated to allow the formation of a film in the dip coating process as well as to increase the strength of the green body (membrane layer before sintering).

All suspensions were prepared by the following method. First, deionized water and the required content of dispersant (Dolapix CE 64) were mixed in a beaker, the fine (Z-1) and the coarse (Z-2) ZrO_2 powders were then added. The suspension was kept under continuous mechanical stirring with a propeller RW 16 (IKA, China) and the pH was adjusted to 10 using a concentrated NH_4OH (30 % NH_3, CAS 1336-21-6, Sigma-Aldrich, USA) solution. Next, the suspension was poured in a polyethylene bottle and milled for 24 h with spherical 9 mm alumina milling beads to ensure homogenization. After the homogenization step, the coating suspension was poured into a beaker and the required amount of binder was added. The mixtures were stirred continuously with a magnetic stirrer at room temperature until the end of the coating process.

The prepared ZrO_2 suspensions were deposited by dip coating on the porous multi-channeled SiC tubular supports using a homemade set-up. In brief, in the case of multi-channel membranes, the suspension was dipped into the channels of the SiC support for 30 s and then pulled out of the suspension at a controlled speed, and in flat sheet membranes the SiC support were dipped into the suspension for 30 s and after that pulled out from the suspension at a controlled speed. Afterwards, the green membranes were dried overnight at 40 °C in a drying cabinet. In the case of double-coated membranes, the dip coating-drying cycle was repeated twice. Once dried, the membranes were sintered in a furnace in air atmosphere. The holding times at the set point temperature were 30 or 1 min. A sintering study was performed to find the optimum temperature to produce good grain joining and appropriate pore size. Own to confidentiality issues, the three different sintering temperatures, in the range between 1000 and 1300 °C, are reported as T−10 °C, T, and T + 50 °C. This temperature range was chosen in order to guarantee the proper ZrO_2 sintering and its adhesion to the SiC support but trying to avoid cracks caused by the volume variation occurring above 1173 °C during the ZrO_2 phase transformation monoclinic→tetragonal [2,5].

Unsupported membranes were prepared from the dried suspensions, sintered under the same conditions above described. The obtained powders were characterized (specific surface area, pore size distribution, and zeta potential) using the same equipment and procedures described in item 2.1.

2.3. Membrane characterization and testing

The morphology, elemental and phase composition of the developed membrane were analysed by SEM, EDS, and XRD according to the same procedures described above. The pore size distributions of the fabricated membranes were analysed by the capillary flow porometry 3 G zh (Quantachrome Instruments, USA). Prior to the measurement, 25 mm long membrane samples were filled with the wetting liquid Porofil™ (Quantachrome Instruments, USA), a fluorinated hydrocarbon with a surface tension of 16 dynes.cm^{-1}. The pore size distribution was calculated from the curves of the airflow through the wet and dry membrane as a function of the air pressure applied with a shape factor of 0.715 measured following the standard ASTM F316_03.

For scratch analyses a TABER 5900 reciprocating abraser (Taber Industries, USA) was utilized equipped with a conical diamond indenter with an angle of 120°, with three different loads and a constant speed of 200 mm min^{-1}. Three scratch tests were done for each load and three measurements of each scratch were done by SEM.

The filtration tests were performed on a commercial pilot scale filtration set-up (Liqtech LabBrain) provided by Liqtech Ceramics A/S (Denmark). This unit consists of a feed tank, a feed pump, a recirculation pump, and a membrane module, as schematically shown in Fig. 1. The membranes were sealed using silicon O-rings and placed in a cross flow stainless-steel module. First, the permeability of the membrane was measured using pure deionized water in order to evaluate its performance at different transmembrane pressure with a cross flow of 1527 L h^{-1} for 10 min. Then, 50 L of feeds with different solutes were filtered in order to evaluate membrane performances in terms of rejection. These experiments were run at a constant transmembrane pressure of 1 bar, and cross flow of 1527 L h^{-1} for 80 min. Recovery factor was set to 90 %. Samples from the feed were taken at the beginning of the experiments while samples from membrane permeate were collected at the end of the experiments. The compounds chosen for retention studies were: hemoglobin, a protein with high molecular weight that is expected to be retained by UF membranes considering their pore size; indigo blue, a dye present in many industrial wastewaters; and humic acid, a model compound for natural organic matter in the water and a model foulant. The hemoglobin concentration in retentates and permeates were determined by size exclusion chromatography (SEC) using an isocratic Agilent 1100 pump (Agilent, CA, USA) equipped with an evaporative light scattering detector ELSD D 2000 (Mandel Scientific, Canada). A gel permeation chromatography (GPC) column (300 × 7.8 mm) PolySep-GFC-P 4000 (Phenomenex, CA, USA) was used with water as the mobile phase, flow rate of 1 mL min-1, and injection volumes of 20 μL. The concentrations of humic acid and indigo blue were determined considering the absorbance of the samples at 254 and 660 nm, respectively, measured with the UV–vis spectrophotometer Cary 50 (Agilent, CA, USA).

Filtration experiments to evaluate the oil removal and possible water reuse were carried out with a simulated oily wastewater. For that, an olive oil/water emulsion was prepared with 500 mg L^{-1} of unprocessed olive oil from the Cooperativa Virgen de la Estrella (Badajoz, Spain) and distilled water. The emulsion was prepared by firstly keeping the oil and the water at high mechanical stirring for 24 h, followed by ultrasonication for 30 min. The stable oil/water emulsion was characterized by measuring droplet size distribution measured by the Dispersion analyser LUMiSizer (LUM GmbH, Germany). Initially, experiments with recirculation of the feed were carried out for determining the critical flux. Then, concentration experiments were performed to separate the olive oil from the water under the optimal condition previously determined. Samples of the feed, retentate and permeate were collected and analysed according to the standards methods for: oil content (ISO 9377-2:2000), total organic carbon (DS/EN 1484:1997), chemical oxygen demand (DS/ISO 15705), and turbidity (DS/EN ISO 7027-1:2016).

Corrosion tests are typically performed in acid and alkaline baths in the pH range of 1−2 and 12–14, respectively [53]. These conditions are more extreme than the ones used in many industrial applications [54]. However, aggressive cleaning conditions, such as high NaOH concentrations, may be used for disinfection and fouling removal [38]. Therefore, highly aggressive conditions were applied in the tests to guarantee that the membranes are not damaged during the cleaning procedures. The corrosion experiments were carried out by placing small pieces of the membrane in two water baths at 60 °C under stirring, one containing 10 %wt of NaOH (pH > 14) and the other 10 %wt of

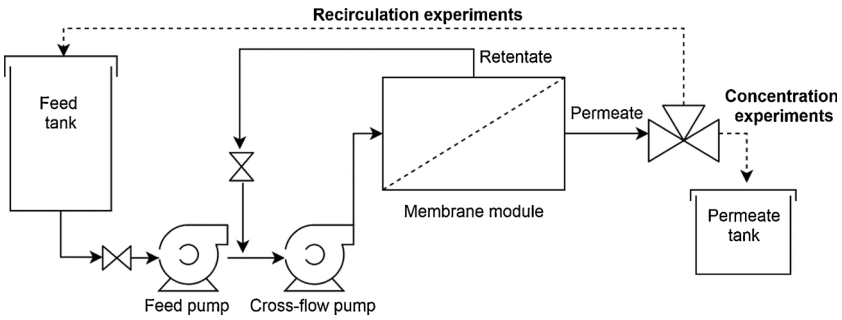

Fig. 1. Schematic diagram of crossflow filtration set-up, Liqtech LabBrain.

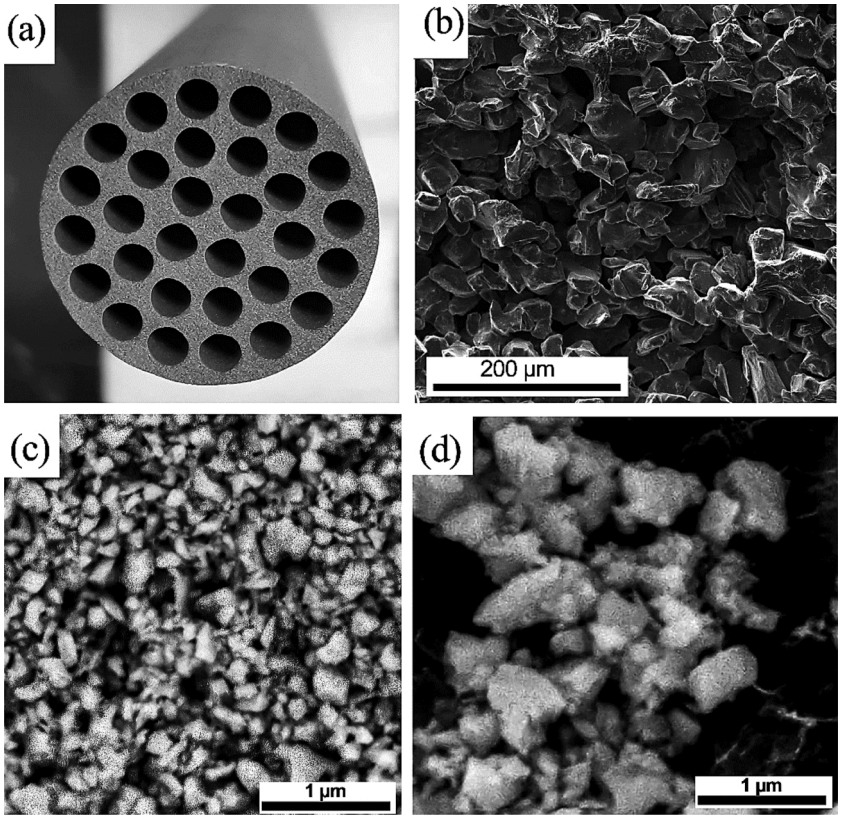

Fig. 2. (a) Multichannel tubular SiC support, (b) SEM image of the silicon carbide tubular support, (c) SEM image of the raw zirconia powder Z-1, (d) SEM image of the raw zirconia powder Z-2.

H_2SO_4 (pH < 0). Samples were collected from each bath every week and characterized by SEM/EDS analysis and pore size distribution.

3. Results and discussion

3.1. Characterization of ZrO_2 powder and SiC support

The two ZrO_2 powders were used as received by the supplier: their particle size distributions were determined by DLS and shown in Fig. S1a. The average particle size of the powders Z-1 and Z-2 are 0.36 and 0.50 µm, respectively. Their specific surface areas, determined by N_2 adsorption-desorption isotherms (Fig. S1b), are presented in Table 1. These powders have specific surface areas around 10 $m^2\ g^{-1}$, as already expected for fused zirconia, *i.e.* obtained at high-temperature arc furnaces [55]. No micro or mesoporosity was observed, the macroporosity responsible for the hysteresis loops observed at very high p/p° values should be mainly caused by the empty spaces between particles. The surface area value of the raw powders can be used to estimate the dosages of dispersants and additives to be added to the slurry in order to obtain a good particle dispersion. It is worthy to notice that the surface

Table 1
Characterization of the raw ZrO_2 powders.

Analysis	Particle size		X-ray Diffraction		Zeta potential		N_2 adsorption
ZrO_2 powder	D_{50} (µm)	D_{90} (µm)	%wt monoclinic	%wt tetragonal	Isoelectric point	ζ-potential at pH 10 (mV)	BET surface area ($m^2\ g^{-1}$)
Z-1	0.32	0.62	99.1	0.9	3.8	−39.4	12.8 ± 0.6
Z-2	0.61	0.98	99.2	0.8	3.5	−36.7	8.5 ± 0.4

area of the final membrane was not evaluated, instead it was determined the pore size distribution.

X-ray diffraction analysis (Fig. S2) with Rietveld refinement demonstrated that the raw powders are composed mainly of monoclinic zirconia with less than 1 %wt of the tetragonal phase (Table 1), in accordance with manufacturer information. Since these ZrO_2 polymorphs have different thermal expansion coefficients, it is important to have a single-phase powder to avoid cracks during sintering of the membrane. The crystallite size of the monoclinic phase are 25 nm and 37 nm for the powders Z-1 and Z-2, respectively. Concerning the morphology of the raw zirconia powders (Fig. 2c and d), both presented relatively round particles, with a size compatible with the ones determined by DLS measurements.

The electrical behaviour of the particles in water was similar for both Z-1 and Z-2 powders (Fig. S1d), for pH values higher than ~4, the particles were negatively charged (Table 1). The surface of ZrO_2 is rich in acid OH groups [56], which explains the negative charge observed increasing the pH.

The silicon carbide supports used for depositing the ZrO_2 layer were homogenous and free of macro-defects (cracks and pinholes), as shown in Fig. 2. According to supplier information, these supports are highly porous (around 40 %) and have average pore size of 15 μm. The support pure water permeability is 12,000 L m^{-2} h^{-1} bar^{-1} [57].

3.2. Optimization of the suspension

For the membrane fabrication by ceramic processing, it is essential to prepare a homogeneous and stable suspension of the starting powders, since well-dispersed particles produce higher average packing densities and a narrower pore size distribution, compared with aggregated suspensions [58] that show different shrinkages during sintering [59]. In order to optimize the ZrO_2 powder suspension, several parameters were investigated, such as the time of ball milling and the dosage of dispersant.

Particles in aqueous media tend to agglomerate because of the ubiquitous attractive van der Waals force between them [51]. A good dispersion requires to balance this force with strong repulsive forces, which can be achieved following three different procedures: i) increasing the charge at the particles surface and/or altering the pH (electrostatic stabilization), ii) adding a polymeric molecule, which is adsorbed onto the powder surface and prevents the particles physically coming close enough (steric stabilization, or iii) applying together these two effects (electrosteric stabilisation) [51,60].

The electrical stabilization generally is obtained when the absolute value of the zeta potential of the colloidal particles is 40 mV or over [60]. Analysing the zeta potential of the ZrO_2 powders (Fig. S1d), the charge is close to −40 mV at pH 10. However, without dispersant, this charge is not enough to ensure a good dispersion of the mix of Z-1 and Z-2 powders, as shown in Fig. 3a, because the negatively charged zirconia particles bind with water molecules by hydrogen bonds, creating a sort of energetic interconnection leading to particle agglomeration [58]. Thus, the addition of a dispersant is necessary.

According to the literature, several compounds can be used to disperse zirconia particles, among others: sodium or ammonium salts of polyacrylic (PAA) or polymethacrylic (PMAA) acids [26,55,61], which are fully dissociated at pH 8.5–9 [62], and carboxylic acid-based polyelectrolyte [24,25,52]. One dispersant of each class was therefore tested for obtaining a stable suspension of the mix of zirconia powders, namely Duramax™ D-3005 (ammonium polyacrylate) and Dolapix CE 64 (carboxylic acid-based). For that, an aqueous dispersion of the ZrO_2 powders, Z-1 and Z-2, with a solid loading of 2.5 %wt, was prepared by ball milling for 24 h. As shown in Fig. 3a, the dispersant Duramax™ D-3005 was not adequate since it led to the formation of agglomerates with a diameter of c.a.10 μm. On the other side, the addition of Dolapix CE 64 led to a reduction of the aggregate size, and thus this dispersant was chosen for further experiments.

Since ball milling was chosen as the method of dispersing the zirconia powders mix, a study of the effect of the time of milling was performed using a solid loading of 2.5 %wt, pH 10, and 2 %wt of Dolapix CE 64. For practical experimental reasons, in the first 8 h of milling,

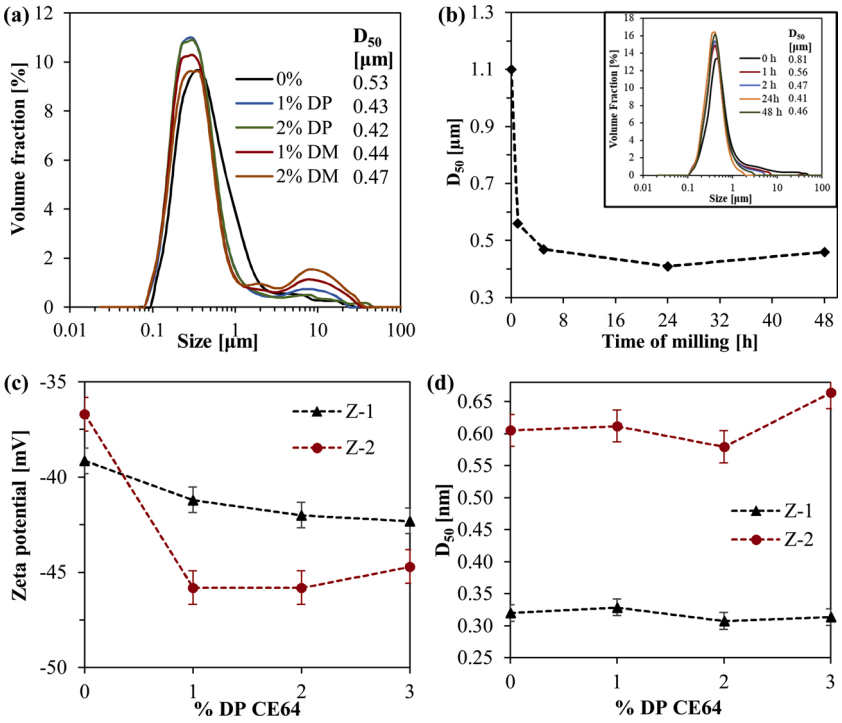

Fig. 3. (a) Particle size distributions for a suspension (2.5 %wt) of the powders Z-1 and Z-2 prepared with different dispersant concentrations (DM: Duramax™ D-3005, DP: Dolapix CE 64), at pH 10 and 24 h of milling; (b) D_{50} of the Z-1 and Z-2 powders suspension after different ball milling times, at pH 10 with 2 %wt of DP. Effects of the dispersant DP dosage on the: (c) zeta potential at pH 10 and (d) D_{50} of the raw zirconia powders at pH 10.

samples were taken every 2 h, then samples were collected after 24 and 48 h. According to Fig. 3b, after 2 h of milling the larger agglomerates disappear, but the best interval time for homogenising the suspension achieving the proper dispersion, avoiding a too large energy consumption, was 24 h, which was chosen for the following of the experiments.

According to a previous work on a zirconia powder dispersion using Dolapix CE 64, the optimal dispersant dosage was around 1 %wt [52]. Therefore, in order to determine the correct dosage of the chosen dispersant for the zirconia used in the present work, zeta potential and particle size of the powders Z-1 and Z-2 were measured for the dispersant concentrations of 1 and 2 %wt. For both powders, the absolute zeta potential value increased to more than 40 mV increasing the dispersant concentration (Fig. 3c), but for the powder Z-2, there was a reduction of the surface charge for concentrations higher than 2 %wt. This suggests that Dolapix CE 64 was adsorbed onto the zirconia surface, so the surface characteristics of the powder were dominated by the features of the polyelectrolyte [51], saturating the particle surface at 2 %wt. of concentration [52]. At the same dispersant concentration, the minimum particle size of the powders was observed (Fig. 3d), whereas a higher concentration seemed to promote flocculation. The dispersant concentration of 2 %wt was therefore chosen for fabricating the membranes.

3.3. Membrane coating and sintering

Once obtained a good suspension, other parameters related to the coating of the support (*e.g.* binders and plasticizers, solid loading, number of coatings) were evaluated for obtaining the smallest pore size possible and a homogeneous and defect-free membrane layer, *i.e.* the basic behaviours for achieving an efficient separation by ceramic membranes [34].

The solid loading was adjusted to obtain a suspension with a specific viscosity that allows dip coating the support to form a homogeneous layer with adequate thickness. Solid loadings of 10, 15, 20, 25, and 30 % wt of the ZrO_2 powder mix (Z-1 and Z-2) were tested. Higher solid loadings led to a great increase of the suspension viscosity, as also reported by other works [52,55]. As a result, it was observed that for solid loadings lower than 20 %wt, no layer was formed after 2 cycles of support coating (Fig. S3a), caused by the excessive infiltration of the coating into the SiC support. The best results were obtained for solid loadings between 25 and 30 %wt and two coating cycles (Table 2). Two coating cycles were chosen in order to obtain a completely formed and non-defective layer (one cycle allowed producing a very thin and non-homogeneous layer, as reported in Fig. S3b), with a good permeability and no cracks (three cycles allowed producing a layer quite thick, low permeable and prone to cracks during drying and/or sintering steps, as shown in Fig. S3c [63]).

In order to improve the film formation during the dip coating process, as well as to increase the green body strength and flexibility, temporary binders were added to the suspension [64]. Organic binders usually burn out above 300 °C and they should burn gradually without leaving ashes. Cellulose-based (*e.g.* carboxyl methylcellulose, hydroxy-propyl cellulose) [34,65], starch-based [66,67], and polyvinyl alcohol (PVA) preparations [26,68–71] are the most used binders for fabricating zirconia membranes. The characterization of the ZrO_2 membranes obtained with the evaluated commercial binders, Optapix PAF 2 (PVA) and Optapix CS 76 (starch-based) are shown in Table 2.

It can be seen that the increase of the binder PAF 2 dosage from 2 to 4 %wt almost doubled the membrane thickness, causing more cracks and increasing the average pore size. This phenomenon is not new, as it is known that thicker layers are more prone to crack because of the critical thickness. In fact, when a wet film containing suspended colloidal particles dries on a substrate, water evaporation causes the adhesion of a film of particles on the substrate, film which resists against the deformation in the plane, although generating tensile stresses [72], only in the case the thickness is limited. Cracks are formed if the tensile stress exceeds a critical value [73] and, in general, there is a critical thickness favouring the spontaneous formation of cracks independently on the drying rate [23]. In addition to this aspect, it is known that PVA produces large pores [74], and in fact the addition of PVA-based PAF 2 caused the formation of very large pores which is disadvantageous for the performance of the membranes in the studied application.

Regarding the membranes obtained with the binder CS 76, they presented smaller thickness and smaller pores than the ones obtained with PAF 2. The optimum binder dosage was 2 %wt, leading to a membrane with the smallest average pore size (64 nm) and the smallest layer thickness (43 ± 3 μm), homogeneous and without cracks. Given the results of these attempts, 2 %wt of CS 76 binder was chosen for fabricating the ZrO_2 membrane on the SiC supports. It can also be observed in Fig. 4 that although the different nature of the materials used as support (SiC) and top layer (ZrO_2), the boundary between them is dense and straight, demonstrating the strong junction between these adjacent layers, for sure improving the membrane lifetime, the resistance to chemical corrosion and water hammering for fouling prevention [34].

Once established the best binder and its dosage, a sintering study was carried out. For confidentiality issues, the sintering temperatures, in the range of 1000–1300 °C, were reported as T−10 °C, T, T + 50 °C. The XRD diffractograms of the membranes sintered at different temperatures and holding times, at these temperatures, of 1 and 30 min, are shown in Fig. 5 and their Rietveld refinements are presented in Table 2.

It can be observed that monoclinic zirconia remained the predominant phase in the membranes after sintering under the different conditions tested. The raw powders contained around 1 %wt of the tetragonal phase (Table 1). However, the increase of the sintering temperature from T−10 to T °C favoured the phase transformation from monoclinic to tetragonal zirconia, as expected considering the tetragonal polymorph is the thermodynamically stable phase at high temperature [59]. On the other hand, for the holding time of 30 min and temperatures of T and T + 50 °C, a decrease of the percentage of the tetragonal zirconia to form a third phase was observed (Fig. S4). The third phase was identified as zirconium silicate ($ZrSiO_4$) and it probably forms in the reaction between the ZrO_2 and small amounts of SiO_2 present in the SiC support at temperatures higher than 900 °C [75,76]. In addition, the crystallite size increased after sintering at high temperatures and long times, as results clearly after treatment at T + 50 °C for 30 min (Table 2 and Fig. 6).

Concerning the morphology of the membranes, it can be seen in Fig. 6 that for sintering temperatures in the range T−10/T °C with 1 min of holding time, grain coarsening mainly occurred, but the volume variation remained low enough to avoid crack generation in the resulting top layer. On the contrary, in the temperature range T/T + 50 °C after 30 min treatment, grain coarsening and densification were observed, the particle size increased and their shape changed to

Table 2
Phase composition and size of the deposited crystals for the membranes sintered at different temperatures and holding times.

Sintering temperature (°C)	Holding time (min)	ZrO_2		Zirconium silicate (%wt)	Crystallite size (m-ZrO_2) (nm)
		Monoclinic (%wt)	Tetragonal (%wt)		
T−10	1	98.0	2.0	0	70
T	1	97.7	2.3	0	77
T	30	97.7	1.7	0.6	98
T + 50	30	98.3	0.6	1.1	228

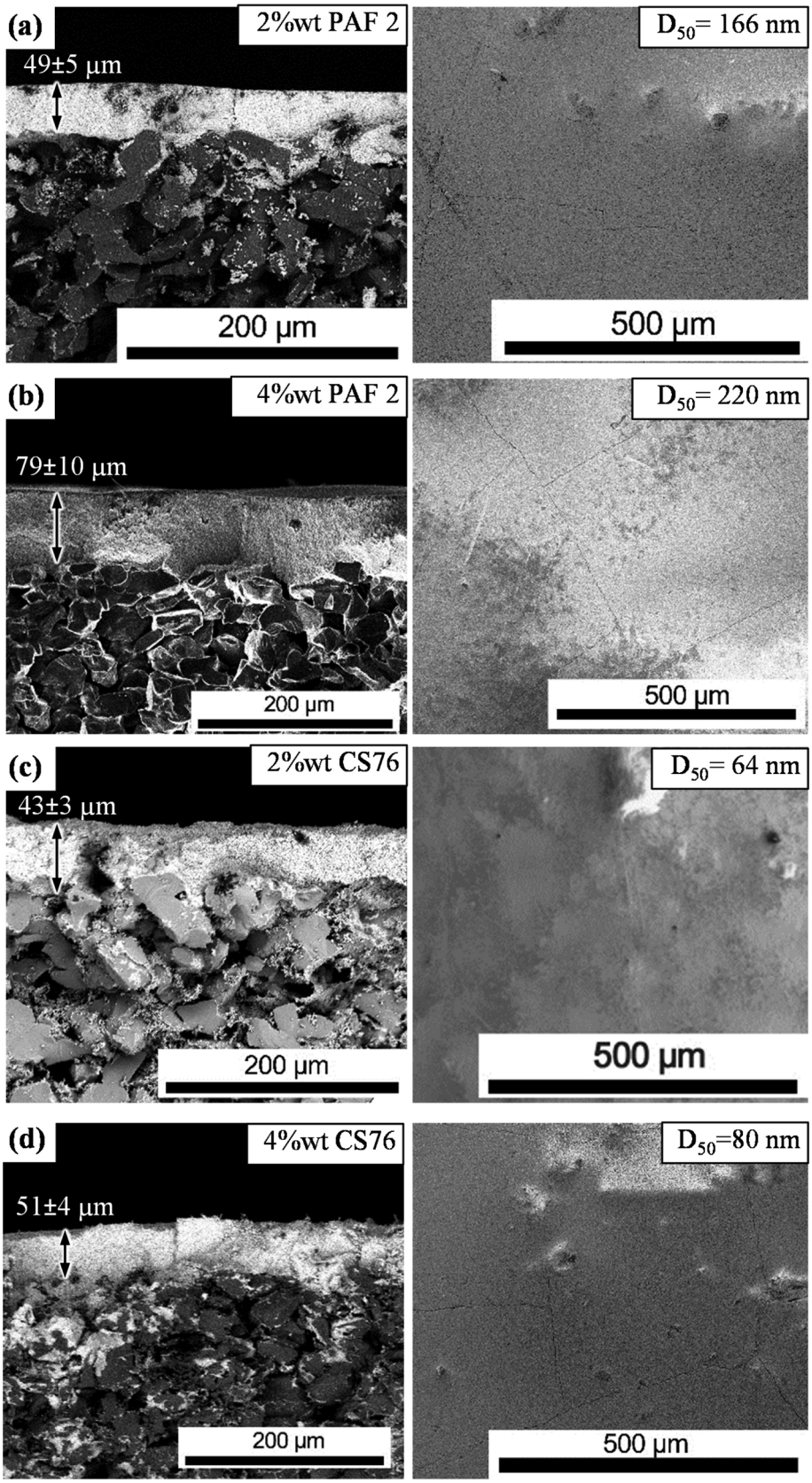

Fig. 4. Membranes obtained with slurries containing (a) 2 and (b) 4 %wt of the binder PAF 2 and (c) 2 and (d) 4 %wt of the binder Optapix CS76 (solid loading = 30 % wt, Dolapix CE 64 = 2 %wt, 24 h of ball milling).

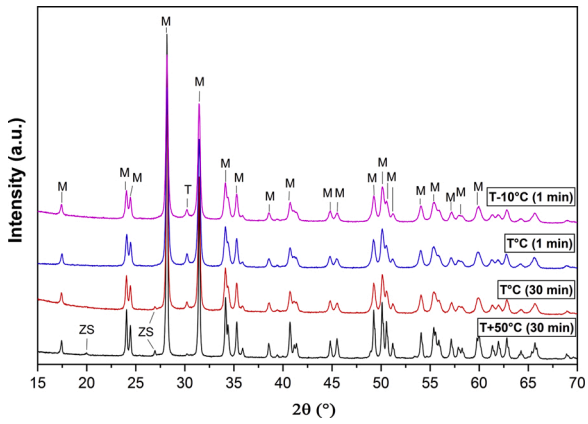

Fig. 5. XRD diffractograms of the membranes sintered under different temperatures and holding times (in brackets). M: monoclinic zirconia, T: tetragonal zirconia, ZS: zirconium silicate.

reduce the surface area [59], with a consequent large dimensional shrinkage responsible for the cracks observed in these membranes (Fig. 6). In addition, the monoclinic phase transformation led to a considerable dimensional variation largely exceeding the maximum stress limit, causing an extensive fragmentation of the layer [59].

Analogous considerations were achieved analysing the pore size distribution (Fig. 7a) of the membranes obtained at different sintering conditions. It can be seen that at T−10 °C, the sintering was not complete since a multimodal distribution of pore sizes is observed. In addition, at this temperature the membrane presented a lower scratch resistance as shown in Fig. 7b. This figure represents the width scratches made on the membrane surface by applying different loads. The smaller the scratch width, the stronger is the top layer mechanical strength and resistance to delamination. Therefore, it can be concluded that the membrane sintered at temperature T for 1 min is the strongest and that the temperatures of T and T + 50 for 30 min led to an excessive crack of the membrane (Fig. 6), which reduces its mechanical strength and causes the larger pore size values observed in Fig. 7a. In conclusion, the optimal sintering condition was at temperature T for 1 min, allowing to complete the sintering of the particles without excessive densification nor phase transformation, resulting in a pore size with a narrow Gaussian distribution and in a mechanically resistant layer.

3.4. Characterization of the membrane

As discussed before, the optimum membrane was obtained using a suspension with 2 %wt of binder (Optapix CS 76), performing two coatings, applying a sintering at T temperature with a holding time of 1 min. The morphological characterization of this membrane was presented in Fig. 6. The top layer is homogeneous, without defects (cracks and pinholes), and it has a thickness of 45 ± 5 μm (Fig. S5a). This membrane also presented an average pore size of 60 nm (Fig. 8a), with D_{50} and D_{90} equal to 58 and 63 nm, respectively. Thus, in order to verify the composition of the developed membrane, EDS analysis was performed on the membrane surface and on its section (Fig. S5). The main elements find in the EDS analysis of the surface (Table S1) were oxygen (21 %wt, 0.62 %mol) and zirconium (77 %wt, 0.38 %mol), indicating that the top layer is composed of pure ZrO_2, which corroborates the XRD results.

Fig. 8b reports the permeate flux obtained for pure water filtration at different transmembrane pressures (TMP). A linear pressure-depended regime (*i.e.* the permeate flux was directly proportional to the TMP applied) was obtained, as expected for pure water (non-fouling) filtration [77]. Under this regime, it was possible to calculate the membrane permeability, which is around 360 L m^{-2} h^{-1} bar^{-1} (LMH/bar). The value obtained is similar to the permeability reported by Li et al. [42] for a zirconia ultrafiltration membrane deposited by a sol-gel route on a silicon support with pore size of 5 μm. On the other hand, by ceramic processing, Li et al. [34] obtained higher clean water permeability values for a 21 μm thick ZrO_2 ultrafiltration membrane obtained on SiC supports. The result is not surprising, as thinner layers allow increasing the permeability, nevertheless in that case an additional intermediate SiC layer, increasing the fabrication cost, was considered. In the present work, a relatively thick ZrO_2 separation layer (45 μm) was required for decreasing the pore size of SiC support (corresponding to15 μm), but no intermediate layer was required [77]. Under this regime, it was possible to calculate the membrane permeability, which is around 360 L m^{-2} h^{-1} bar^{-1} (LMH/bar). The value obtained is similar to the permeability reported by Li et al. [42] for a zirconia ultrafiltration membrane deposited by a sol-gel route on a silicon support with pore size of 5 μm. On the other hand, by ceramic processing, Li et al. [34] obtained higher clean water permeability values for a 21 μm thick ZrO_2 ultrafiltration membrane obtained on SiC supports. The result is not surprising, as thinner layers allow increasing the permeability, nevertheless in that case an additional intermediate SiC layer, increasing the fabrication cost, was considered. In the present work, a relatively thick ZrO_2 separation layer (45 μm) was required for decreasing the pore size of SiC support (corresponding to15 μm), but no intermediate layer was required.

Concerning the retention properties of the membranes, there are some parameters that determines if a compound is retained or not, namely the type of membranes (*e.g.* UF, NF, RO), the properties of the compound (*e.g.* molecular weight and size, acid dissociation constant, hydrophobicity/hydrophilicity, diffusion coefficient, charge), and the operation conditions (flow, temperature, pH) [78]. For ultrafiltration membranes, there are four mechanisms of retention: size exclusion, adsorption, hydrophobic interactions, and electrostatic interactions [79]. Therefore, it was selected some compounds with different sizes and chemical properties for evaluating the developed membrane. The retention of these compounds is presented on Table 3. Large molecules such as humic acid and hemoglobin can be easily separated, as expected considering their large size and the repulsion between their negative charge and the negatively charged ZrO_2 particles forming the filtering layer (see the zeta potential of the unsupported powder in Fig. S1d). However, also indigo blue, a quite small molecule, has a high retention, even higher than hemoglobin one, probably because its high adsorption to the membrane surface (visually observed) and due to the fact that this compound is scarcely soluble in water and forms micelles that can be easily retained by the membrane. In conclusion, the membrane under study is efficient in removing contaminants different in nature and this suggests they do not separate for simple sieving effect, but probably electrostatic interactions and dispersion forces can play additional and significant roles [79]. In order to evaluate these roles, also oil/water separation trials were performed taking advantage of the high hydrophilicity of zirconia [80].

These oil/water emulsions were prepared with 1000 mg L^{-1} of motor oil or crude oil from the North Sea and 100 mg L^{-1} of the surfactant Tween 80. As a result, 91 % of motor oil and 84 % of crude oil were removed. The good results obtained indicated that this membrane is also efficient for the treatment of wastewaters containing oil, such as effluents from petrochemical and metallurgical industries, as well as cosmetics and food production, tanning and leather processing [80]. Therefore, more tests were carried out in real conditions for the recovery of olive oil from water.

3.5. Olive oil recovery (oil/water separation)

The olive oil/water emulsion prepared by ultrasonication was stable for several days and presented an average droplet size of 1.35 μm with the oil droplets between the limit of 0.3 and 2.7 μm (Fig. S6a).

Prior to the actual olive oil/water emulsion filtration, the critical permeate flux should be determined in order to minimize the fouling

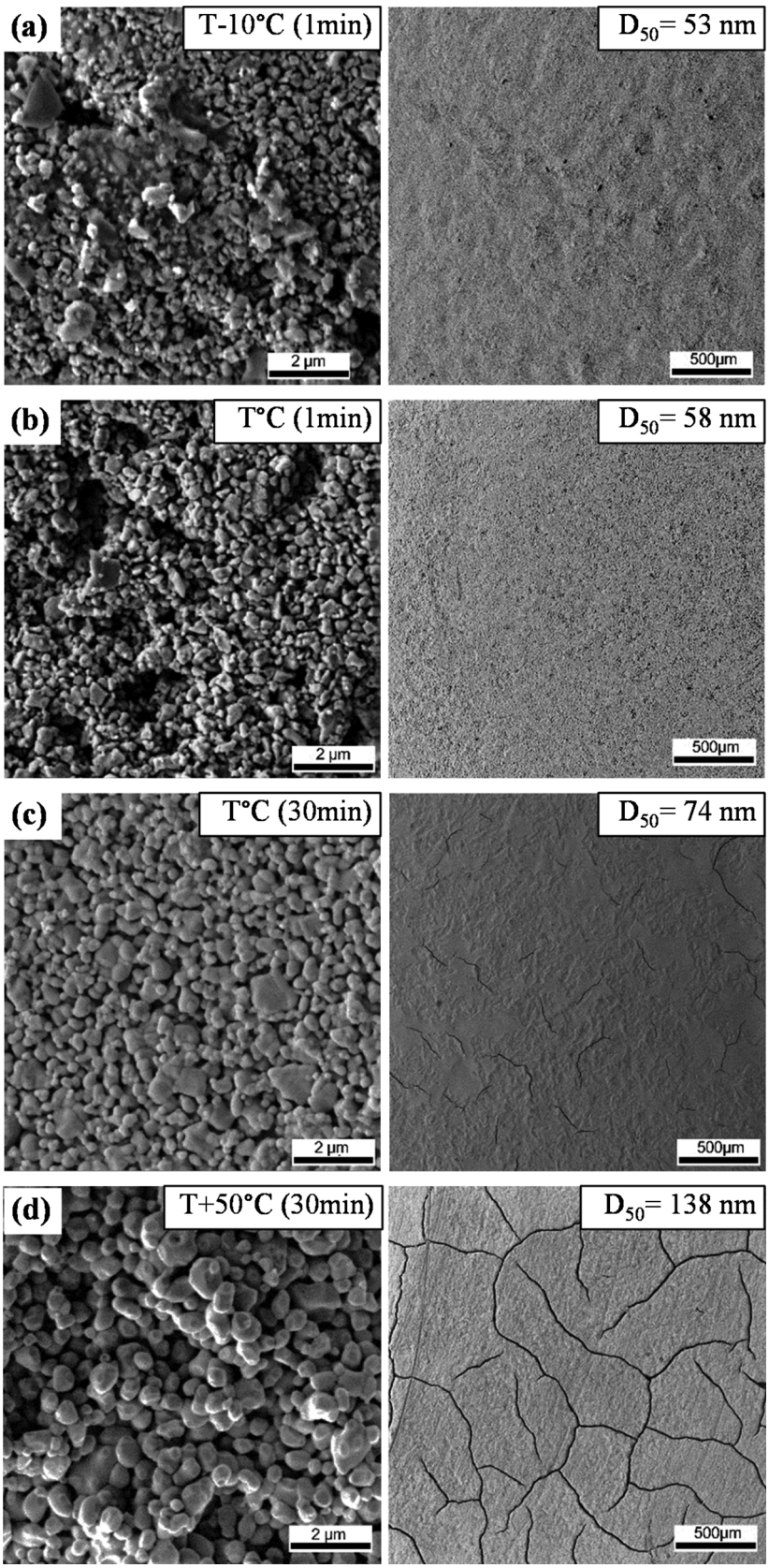

Fig. 6. SEM images of the surface of the membranes and their respective pore size (D_{50}) for the sintering conditions of (a) T−10 °C for 1 min, (b) T °C for 1 min, (c) T °C for 30 min, (d) T + 50 °C for 30 min.

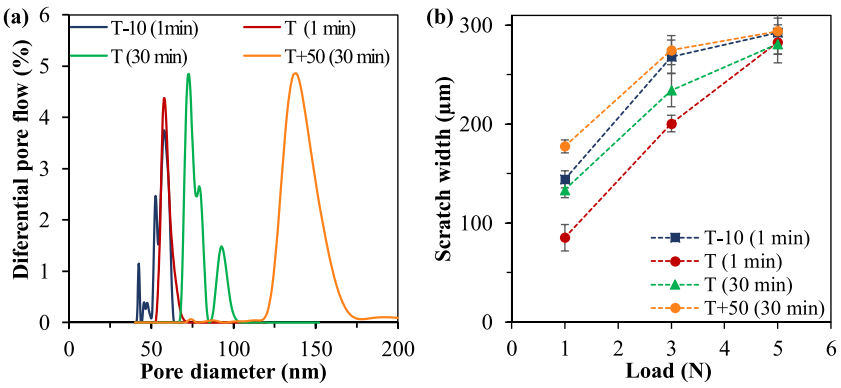

Fig. 7. Effect of the sintering temperatures and holding time on the: (a) pore size distribution and (b) scratch width for different loads applied.

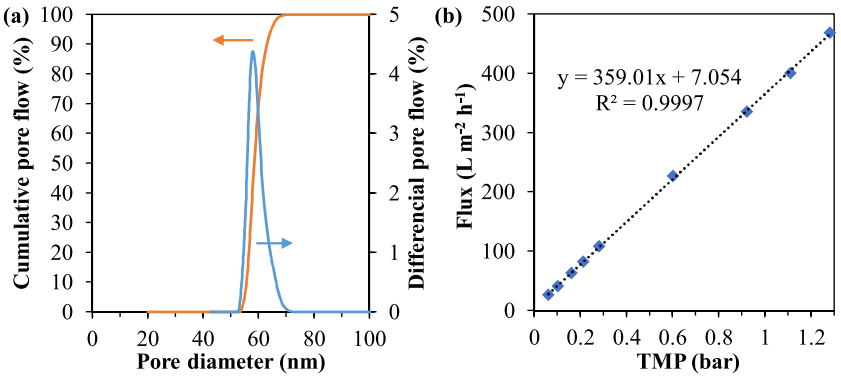

Fig. 8. (a) Pore size distribution of the ZrO_2/SiC membrane. (b) Pure water flux at different transmembrane pressures (TMP).

Table 3
Retention of selected compounds and oil removal of oil in water emulsions prepared with different oils.

Compound	MW (kDa)	Isoelectric point [81, 82,83]	Charge at pH 7	Retention (%)
Humic Acid	4.7–30.4	3	negative	98 ± 2
Indigo blue	0.262	N.A.	neutral	88 ± 1
Hemoglobin	64.5	5–7	negative	82 ± 3
Oil/Water emulsion with				Oil removal (%)
Motor oil				91 ± 4
Crude oil (North sea)				84 ± 3

during the emulsion filtration. For that, experiments were carried out with the recirculation of the permeate by setting constant permeate flowrates and assessing the variation of transmembrane pressure (TMP) for intervals of 15 min (Fig. S6b). The permeate flux was plotted according to the TMP (Fig. 9a): the trend observed allowed to evidence the critical flux (150 L m^{-2} h^{-1}), *i.e.* the maximum flux that can be applied without causing significant fouling.

Once determined the critical flux, filtration experiments (with no recirculation of the permeate) were performed to promote the olive oil separation from the emulsion with a permeate flux of 90 L m^{-2} h^{-1}. The transmembrane pressure during this test was recorded (Fig. S7) and used to calculate the water permeability, which was around 300 L m^{-2} h^{-1} bar^{-1}. As show in Fig. 9b, no considerable fouling was observed during the filtration of olive oil/water emulsion and therefore the permeability was almost constant. The analysis of the feed, retentate and permeate

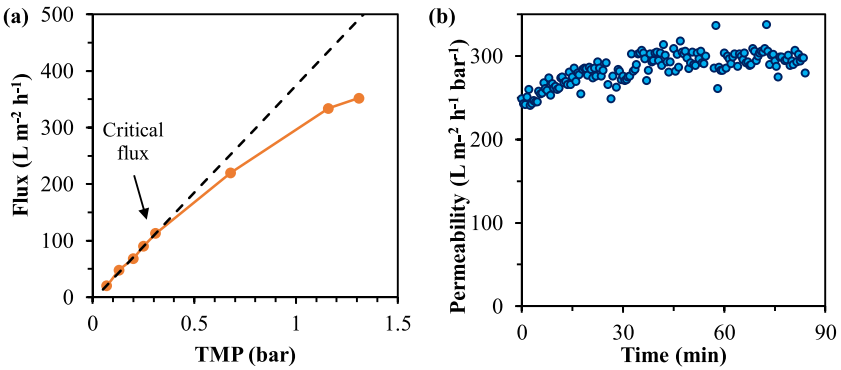

Fig. 9. (a) Permeate flux as a function of the transmembrane pressure (TMP) applied in the filtration under recirculation. The arrow indicates the critical flux. (b) Permeability obtained in the oil/water separation experiments with a permeate flux of 90 L m^{-2} h^{-1}.

Table 4
Characteristics of the feed, retentate and permeate obtained in the olive oil/water emulsion filtration under the optimal condition.

	Feed	Retentate	Permeate	Removal (%)
COD (mg L^{-1})	1430	13,024	10.3	99.28
TOC (mg L^{-1})	35	311	1.2	96.57
Turbidity (NTU)	89	253	1.1	98.76
Oil Content	500	4895	0.45	99.91

are shown in Table 4.

As it can be observed, a removal of 99.91 % of olive oil was achieved, implying in high removals of COD (chemical oxygen demand), TOC (total organic carbon), and turbidity, which would allow the water reuse or its disposal into watercourses according to European regulations [36]. Moreover, a retentate with a concentration factor of 9.8 was obtained, which could be processes for recovering the olive oil. In Table 5, it is presented a comparison between the membrane developed in this work and other membranes tested for oil/water separation.

As it can be seen in this table, high retentions of oil were reported by other authors, but in most of those works, the permeate flux is lower than the ones obtained with the membranes here developed. For instance, Yang et al. [21] obtained 99.8 % of oil rejection with a ZrO_2 membrane, on a α-Al_2O_3 support, with pore size of 0.2 μm, but with a permeability of the membrane of 97 L m^{-2} h^{-1} bar^{-1}, much lower than the 300 L m^{-2} h^{-1} bar^{-1} obtained with our ZrO_2/SiC membrane. Fraga et al. [36] tested pure SiC UF membranes but still the permeate flux was moderate. The reason for the high water permeability achieved in the present work is the unique combination of the highly porous and super hydrophilic SiC support with the ZrO_2 that is also highly hydrophilic. Although Zhou et al. [48] observed a higher permeate flux, these authors utilized a microfiltration membrane, with pores size much larger than the ones reported in the present work. In addition, a great part of the membranes applied for the oil/water separation are made of alumina (or use alumina supports), which do not have the high chemical and mechanical resistance [31] of the developed ZrO_2/SiC membrane.

3.6. Corrosion

The main advantage in using a SiC support with a ZrO_2 selective layer for fabricating an ultrafiltration membrane stands in the fact that both components have outstanding chemical, thermic and mechanical resistances. In order to verify the membrane resistance to highly acid and alkaline media, samples were submerged for several weeks under NaOH and H_2SO_4 solutions. As it can be seen in Fig. 10, the pore size distribution, expressed by the D_{90} of the membranes, remained almost unaffected by the treatments, indicating that the membrane is resistant to acid and alkaline corrosion under the harsh conditions tested.

With the purpose of verifying these results, SEM imaging with EDS analysis were performed in the samples. As it can be seen in Table 6, the chemical composition of the membranes did not suffer relevant reduction of the Zr percentage, as expected for this material [86]. Furthermore, the EDS probe only detect the elements Zr, O, Si, and C (Fig. S8), confirming that the zirconia layer is chemically inert to H_2SO_4 and NaOH under the conditions tested. Although a small reduction of the C and Si amounts was noticed after the acid and alkaline baths, these changes should be related to the removal of residual C and SiO_2 present in the SiC support [57,87]. In addition, no significant changes were observed in the morphology of the samples after the corrosion tests, as shown in Fig. 11. Other authors [18] reported similar results for zirconia membranes, even after treatment in hydrothermal conditions.

In order to summarize the results obtained in this work and compare the performance of the ZrO2 membrane here developed, it was elaborated Table 7 with the few UF zirconia membranes reported in literature.

From this table, it can be observed that the largest part of zirconia membranes is fabricated on alumina supports, which does not have the high chemical stability of the silicon carbide used in the present work [16,31]. In addition, our ZrO_2/SiC has higher water permeability in comparison to ZrO_2/Al_2O_3 membranes with similar pore size. Even though Li et al. [34] fabricated a ZrO_2 membrane using ceramic processing on SiC supports, achieving a really high water permeability, these authors needed an intermediate SiC layer before the top ZrO_2 layer, which increases the fabrication cost. On the other hand, Li et al. [42] used a sol-gel method for the direct deposition of Y-ZrO_2 layer on a SiC support but this process is more complex, expensive and has a larger footprint. In addition, yttria-doped zirconia does not have the same thermal stability of the monoclinic ZrO_2 used in this work, since yttrium can be easily leached in acid environment, with consequent destabilization of the material [16,86]. In summary, the membranes developed in the present work stands up for being fabricated by ceramic processing on SiC supports and guaranteeing corrosion resistance and high water permeability.

Table 5
Comparison of different membranes applied in oil/water separation.

Reference	Type	Composition	Initial Oil concentration (mg L^{-1})	Water permeability (L. m^{-2}. h^{-1}. bar^{-1})	Oil removal
Present work	UF	ZrO_2/SiC	500	300	99.91
Fraga et al. [36]	UF	SiC	275	130	99
Eom et al. [49]	MF	Clay modified with Carbon black	100	216	96.7
Zhang et al. [84]	NF	S-Y-ZrO_2/PSF	80	110	99.16
Zhou et al. [48]	MF	Al_2O_3 modified with ZrO_2	1000	750	97–99.2
Chang et al. [85]	MF	Al_2O_3 modified with Al_2O_3	1000	250	98.5
Yang et al. [21]	MF	ZrO_2/Al_2O_3	5000	93	99.8

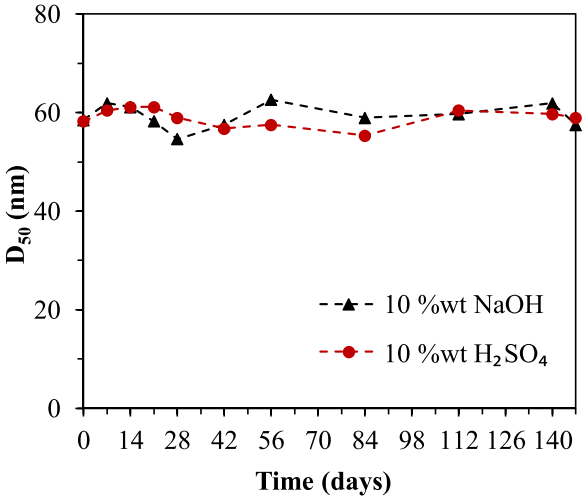

Fig. 10. D_{50} (diameter in which 50 % of the pores are below this value) of the membranes subjected to acid and basic corrosion tests.

Table 6
EDS elemental analysis of the membrane before and after 142 days in the acid and alkaline baths.

Element	Weight percentage (%)		
	Membrane after sintering	10 % H_2SO_4	10 % NaOH
Zr	76.9 ± 2.2	76.8 ± 1.9	76.6 ± 2.1
O	21.5 ± 1.3	21.9 ± 1.5	22.0 ± 1.7
C	0.9 ± 0.1	0.6 ± 0.1	0.8 ± 0.1
Si	0.7 ± 0.1	0.7 ± 0.1	0.6 ± 0.2
Na	N.D.	N.D.	N.D.
S	N.D.	N.D.	N.D.

N.D. = non-detected.

4. Conclusions

In the present work, an ultrafiltration composite membrane made of monoclinic zirconia on silicon carbide supports was developed. The optimised formulation allows to maintain the high mechanical-chemical properties of SiC, but also to reduce production costs in comparison with pure SiC UF membranes, since zirconia can be sintered in air at lower temperatures than SiC. The composite membrane was manufactured by coating a high porous SiC support with a zirconia particles slurry prepared by ceramic processing. The optimum slurry was obtained with the aid of 2 %wt of the dispersant Dolapix CE 64 followed by ball milling for 24 h and addition of 2 %wt of the binder Optapix CS 76. With two dip coating-drying cycles, a homogenous and defect free separation layer was obtained on top of the SiC supports. The green membranes were calcined in a temperature range between 1000 and 1300 °C in air, obtaining a pore size around 60 nm and a pure water permeability of

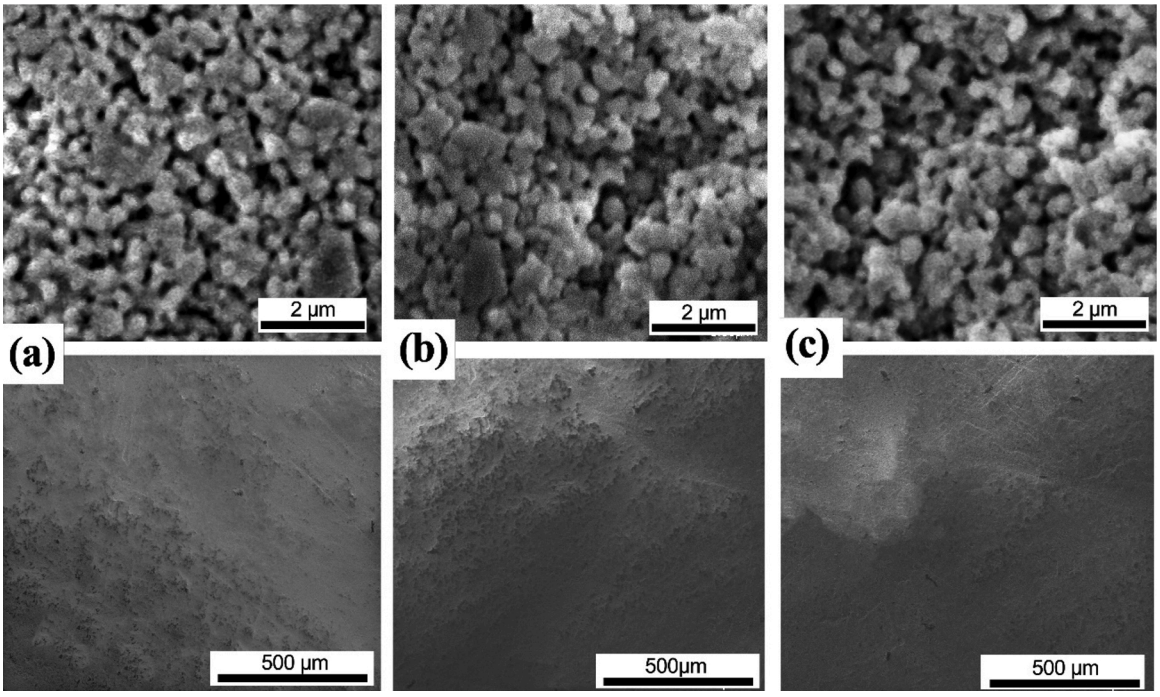

Fig. 11. SEM images of the membrane (a) before the corrosion test and after 142 days in the (a) acid bath and (b) alkaline bath.

Table 7
Comparison of ultrafiltration zirconia membranes.

Reference	Preparation method	Support		Top layer		Sintering Temperature (°C)	Average Pore size (nm)	Water Permeability (LMH. bar^{-1})
		Type	Pore size (µm)	Composition	Thickness (µm)			
This work	Particle suspension	SiC	15	Monoclinic ZrO_2	45	1000- 1300	60	360
Li et al. [42]	Sol-gel	SiC	5	Tetragonal Y-ZrO_2	60	700 800 900	63 57 48	355 302 273
Li et al. [34]	Particle suspension	I- SiC II- SiC	I- 1-2 II- 0.9	Monoclinic/ Tetragonal ZrO_2	21	800 900 1000	82 67 45	708 658 737
Dey et al. [24]	Particle suspension	Clay-Al_2O_3	0.8	Tetragonal Y-ZrO_2	3	700	40	48

Commercial membranes

Company	Product	Support	Top layer composition	Average pore size (nm)
Pall Food and Drink	Membralox®	α-Al_2O_3	ZrO_2	20; 50; 100
TAMI industries	INSIDE CéRAM™	α-Al_2O_3	ZrO_2	5 to 30
Inopor	inopor® ultra	α-Al_2O_3	ZrO_2	3; 110

360 L m^{-2} h^{-1} bar^{-1} after treatment at the optimal temperature. The membrane presented good retention of humic acid, indigo dye, and hemoglobin, which indicated the possibility to use this membrane in treating wastewater containing organic matter, from tanning and food industries. In a real application the membrane was able to remove 99.91 % of oil from an olive oil/water emulsion, reducing TOC, COD, and turbidity values, which would allow the water reuse. Finally, the developed membrane is mechanically strong and resistant to corrosion at basic and acid baths without changing the pore size during the time. These results indicates that the ZrO_2/SiC membrane has potential to operate in harsh conditions, such as for the treatment of heavily contaminated industrial effluents, or in food applications that require severe membrane cleaning.

Declaration of Competing Interest

The authors declare that they have no known competing financial interests or personal relationships that could have appeared to influence the work reported in this paper.

Acknowledgments

This paper is part of a project that has received funding from the European Union's Horizon 2020 research and innovation programme under the Marie Skłodowska-Curie grant agreement No 765860.

Appendix A. Supplementary data

Supplementary material related to this article can be found, in the online version, at doi:https://doi.org/10.1016/j.jeurceramsoc.2021.07.054.

References

[1] A. Boulkrinat, F. Bouzerara, A. Harabi, K. Harrouche, S. Stelitano, F. Russo, F. Galiano, A. Figoli, Synthesis and characterization of ultrafiltration ceramic membranes used in the separation of macromolecular proteins, J. Eur. Ceram. Soc. (2020), https://doi.org/10.1016/j.jeurceramsoc.2020.06.060.
[2] D. da Silva Biron, V. dos Santos, M. Zeni, Ceramic Membranes Applied in Separation Processes, 2018, https://doi.org/10.1007/978-3-319-58604-5.
[3] Z. He, Z. Lyu, Q. Gu, L. Zhang, J. Wang, Ceramic-based membranes for water and wastewater treatment, Colloids Surf. A Physicochem. Eng. Asp. 578 (2019), 123513, https://doi.org/10.1016/j.colsurfa.2019.05.074.
[4] Y. Zhu, D. Wang, L. Jiang, J. Jin, Recent progress in developing advanced membranes for emulsified oil/water separation, NPG Asia Mater. 6 (2014) e101, https://doi.org/10.1038/am.2014.23.
[5] V. Gitis, G. Rothenberg, Ceramic Membranes: New Opportunities and Practical Applications, John Wiley & Sons, 2016.
[6] S. Benfer, U. Popp, H. Richter, C. Siewert, G. Tomandl, Development and characterization of ceramic nanofiltration membranes, Sep. Purif. Technol. 22–23 (2001) 231–237, https://doi.org/10.1016/S1383-5866(00)00133-7.
[7] R. Allabashi, M. Arkas, G. Hörmann, D. Tsiourvas, Removal of some organic pollutants in water employing ceramic membranes impregnated with cross-linked silylated dendritic and cyclodextrin polymers, Water Res. 41 (2007) 476–486, https://doi.org/10.1016/j.watres.2006.10.011.
[8] M.J.H. Snow, D. de Winter, R. Buckingham, J. Campbell, J. Wagner, New techniques for extreme conditions: high temperature reverse osmosis and nanofiltration, Desalination 105 (1996) 57–61, https://doi.org/10.1016/0011-9164(96)00058-6.
[9] X. Da, X. Chen, B. Sun, J. Wen, M. Qiu, Y. Fan, Preparation of zirconia nanofiltration membranes through an aqueous sol–gel process modified by glycerol for the treatment of wastewater with high salinity, J. Memb. Sci. 504 (2016) 29–39, https://doi.org/10.1016/j.memsci.2015.12.068.
[10] Y. Lu, T. Chen, X. Chen, M. Qiu, Y. Fan, Fabrication of TiO2-doped ZrO2 nanofiltration membranes by using a modified colloidal sol-gel process and its application in simulative radioactive effluent, J. Memb. Sci. 514 (2016) 476–486, https://doi.org/10.1016/j.memsci.2016.04.074.
[11] T. Tsuru, Inorganic porous membranes for liquid phase separation, Sep. Purif. Methods 30 (2001) 191–220, https://doi.org/10.1081/SPM-100108159.
[12] A. Kayvani Fard, G. McKay, A. Buekenhoudt, H. Al Sulaiti, F. Motmans, M. Khraisheh, M. Atieh, Inorganic membranes: preparation and application for water treatment and desalination, Materials 11 (2018) 74, https://doi.org/10.3390/ma11010074.
[13] A. Basile, F. Gallucci, Membranes for Membrane Reactors: Preparation, Optimization and Selection, John Wiley & Sons, 2010.
[14] T. van Gestel, D. Sebold, Hydrothermally stable mesoporous ZrO 2 membranes prepared by a facile nanoparticle deposition process, Sep. Purif. Technol. 221 (2019) 399–407, https://doi.org/10.1016/j.seppur.2019.03.066.
[15] H. Verweij, Inorganic membranes, Curr. Opin. Chem. Eng. 1 (2012) 156–162, https://doi.org/10.1016/j.coche.2012.03.006.
[16] T. van Gestel, C. Vandecasteele, A. Buekenhoudt, C. Dotremont, J. Luyten, B. van der Bruggen, G. Maes, Corrosion properties of alumina and titania NF membranes, J. Memb. Sci. 214 (2003) 21–29, https://doi.org/10.1016/S0376-7388(02)00517-3.
[17] T. Van Gestel, D. Sebold, H. Kruidhof, H.J.M. Bouwmeester, ZrO2 and TiO2 membranes for nanofiltration and pervaporation. Part 2. Development of ZrO2 and TiO2 toplayers for pervaporation, J. Memb. Sci. 318 (2008) 413–421, https://doi.org/10.1016/j.memsci.2008.03.003.
[18] T. Van Gestel, H. Kruidhof, D.H.A. Blank, H.J.M. Bouwmeester, ZrO2 and TiO2 membranes for nanofiltration and pervaporation Part 1. Preparation and characterization of a corrosion-resistant ZrO2 nanofiltration membrane with a MWCO<300, J. Memb. Sci. 284 (2006) 128–136, https://doi.org/10.1016/j.memsci.2006.07.020.
[19] M.A. Rahman, M. Ha, D. Othman, A.F. Ismail, Morphological study of yttria-stabilized zirconia hollow fibre membrane prepared using phase inversion / sintering technique, Ceram. Int. 41 (2015) 12543–12553, https://doi.org/10.1016/j.ceramint.2015.06.066.
[20] S. Anisah, W. Puthai, M. Kanezashi, H. Nagasawa, T. Tsuru, Preparation, characterization, and evaluation of TiO2-ZrO2 nanofiltration membranes fired at different temperatures, J. Memb. Sci. 564 (2018) 691–699, https://doi.org/10.1016/j.memsci.2018.07.072.
[21] C. Yang, G. Zhang, N. Xu, J. Shi, Preparation and application in oil–water separation of ZrO2/α-Al2O3 MF membrane, J. Memb. Sci. 142 (1998) 235–243, https://doi.org/10.1016/S0376-7388(97)00336-0.
[22] R.S. Faibish, Y. Cohen, Fouling and rejection behavior of ceramic and polymer-modified ceramic membranes for ultrafiltration of oil-in-water emulsions and microemulsions, Colloids Surf. A Physicochem. Eng. Asp. 191 (2001) 27–40, https://doi.org/10.1016/S0927-7757(01)00761-0.
[23] M. Qiu, Y. Fan, N. Xu, Preparation of supported zirconia ultrafiltration membranes with the aid of polymeric additives, J. Memb. Sci. 348 (2010) 252–259, https://doi.org/10.1016/j.memsci.2009.11.009.
[24] S. Dey, P. Bhattacharya, S. Bandyopadhyay, S.N. Roy, S. Majumdar, G.C. Sahoo, Single step preparation of zirconia ultrafiltration membrane over clay-alumina based multichannel ceramic support for wastewater treatment, J. Membr. Sci. Res. 4 (2018) 28–33, https://doi.org/10.22079/jmsr.2017.58311.1126.
[25] N. Saffaj, R. Mamouni, A. Laknifli, A. Mouna, S.A. Younssi, A. Albizane, Efficiency of ultrafiltration ceramic membranes for toxic elements removal from wastewaters, scientific study & research, Ind. Eng. Chem. Chem. Eng. Data Ser. 11 (2010) 243–254.
[26] F. Shojai, T.A. Mäntylä, Effect of sintering temperature and holding time on the properties of 3Y-ZrO2 microfiltration membranes, J. Mater. Sci. 36 (2001) 3437–3446, https://doi.org/10.1023/A:1017908011672.
[27] H. Qin, W. Guo, X. Huang, P. Gao, H. Xiao, Preparation of yttria-stabilized ZrO2 nanofiltration membrane by reverse micelles-mediated sol-gel process and its application in pesticide wastewater treatment, J. Eur. Ceram. Soc. 40 (2020) 145–154, https://doi.org/10.1016/j.jeurceramsoc.2019.09.023.
[28] H. Guo, S. Zhao, X. Wu, H. Qi, Fabrication and characterization of TiO 2 /ZrO 2 ceramic membranes for nanofiltration, Microporous Mesoporous Mater. 260 (2018) 125–131, https://doi.org/10.1016/j.micromeso.2016.03.011.
[29] W. Deng, X. Yu, M. Sahimi, T.T. Tsotsis, Highly permeable porous silicon carbide support tubes for the preparation of nanoporous inorganic membranes, J. Memb. Sci. 451 (2014) 192–204, https://doi.org/10.1016/j.memsci.2013.09.059.
[30] M. Facciotti, V. Boffa, G. Magnacca, L.B. Jørgensen, P.K. Kristensen, A. Farsi, K. König, M.L. Christensen, Y. Yue, Deposition of thin ultrafiltration membranes on commercial SiC microfiltration tubes, Ceram. Int. 40 (2014) 3277–3285, https://doi.org/10.1016/j.ceramint.2013.09.107.
[31] E. Eray, V.M. Candelario, V. Boffa, H. Safafar, D.N. Østedgaard-Munck, N. Zahrtmann, H. Kadrispahic, M.K. Jørgensen, A roadmap for the development and applications of silicon carbide membranes for liquid filtration: Recent advancements, challenges, and perspectives, Chem. Eng. J. 414 (2021), 128826, https://doi.org/10.1016/j.cej.2021.128826.
[32] M.C. Fraga, S. Sanches, V.J. Pereira, J.G. Crespo, L. Yuan, J. Marcher, M.M. de Yuso, E. Rodríguez-Castellón, J. Benavente, Morphological, chemical surface and filtration characterization of a new silicon carbide membrane, J. Eur. Ceram. Soc. 37 (2017) 899–905, https://doi.org/10.1016/j.jeurceramsoc.2016.10.007.
[33] B.J. Lee, Z. Zhang, S. Baek, S. Kim, D. Kim, K. Yong, Bio-inspired dewetted surfaces based on SiC/Si interlocked structures for enhanced-underwater stability and regenerative-drag reduction capability, Sci. Rep. 6 (2016) 24653, https://doi.org/10.1038/srep24653.
[34] S. Li, C. Wei, P. Wang, P. Gao, L. Zhou, G. Wen, Zirconia ultrafiltration membranes on silicon carbide substrate: microstructure and water flux, J. Eur. Ceram. Soc. 40 (2020) 4290–4298, https://doi.org/10.1016/j.jeurceramsoc.2020.04.020.
[35] N. Li, X. Wang, H. Zhang, Z. Zhang, J. Ding, J. Lu, Comparing the performance of various nanofiltration membranes in advanced oxidation-nanofiltration treatment of reverse osmosis concentrates, Environ. Sci. Pollut. Res. - Int. 26 (2019) 17472–17481, https://doi.org/10.1007/s11356-019-05120-2.
[36] M. Fraga, S. Sanches, J. Crespo, V. Pereira, Assessment of a new silicon carbide tubular honeycomb membrane for treatment of olive mill wastewaters, Membranes 7 (2017) 12, https://doi.org/10.3390/membranes7010012.

[37] R. Neufert, M. Moeller, A.K. Bakshi, Dead-End Silicon Carbide Micro-Filters for Liquid Filtration, 2013, pp. 113–125, https://doi.org/10.1002/9781118807811.ch10.
[38] B. Hofs, J. Ogier, D. Vries, E.F. Beerendonk, E.R. Cornelissen, Comparison of ceramic and polymeric membrane permeability and fouling using surface water, Sep. Purif. Technol. 79 (2011) 365–374, https://doi.org/10.1016/j.seppur.2011.03.025.
[39] R.J. Ciora, B. Fayyaz, P.K.T. Liu, V. Suwanmethanond, R. Mallada, M. Sahimi, T. T. Tsotsis, Preparation and reactive applications of nanoporous silicon carbide membranes, Chem. Eng. Sci. 59 (2004) 4957–4965, https://doi.org/10.1016/j.ces.2004.07.015.
[40] M. Xu, M. Guan, S. Wang, M. Wu, Preparation of Silicon Carbide hollow fiber membrane in low temperature by precursor pyrolysis, IOP Conf. Ser.: Mater. Sci. Eng. 768 (2020), 022061, https://doi.org/10.1088/1757-899X/768/2/022061.
[41] Q. Jiang, J. Zhou, Y. Miao, S. Yang, M. Zhou, Z. Zhong, W. Xing, Lower-temperature preparation of SiC ceramic membrane using zeolite residue as sintering aid for oil-in-water separation, J. Memb. Sci. 610 (2020), 118238, https://doi.org/10.1016/j.memsci.2020.118238.
[42] S. Li, C. Wei, L. Zhou, P. Wang, Q. Meng, Z. Xie, Sol-gel derived zirconia membrane on silicon carbide substrate, J. Eur. Ceram. Soc. (2019) 0–1, https://doi.org/10.1016/j.jeurceramsoc.2019.04.054.
[43] H. Qi, G. Zhu, L. Li, N. Xu, Fabrication of a sol–gel derived microporous zirconia membrane for nanofiltration, J. Solgel Sci. Technol. 62 (2012) 208–216, https://doi.org/10.1007/s10971-012-2711-0.
[44] T. Okubo, T. Takahashi, M. Sadakata, H. Nagamoto, Crack-free porous YSZ membrane via controlled synthesis of zirconia sol, J. Memb. Sci. 118 (1996) 151–157, https://doi.org/10.1016/0376-7388(96)00085-3.
[45] Y. Zhou, M. Fukushima, H. Miyazaki, Y. ichi Yoshizawa, K. Hirao, Y. Iwamoto, K. Sato, Preparation and characterization of tubular porous silicon carbide membrane supports, J. Memb. Sci. 369 (2011) 112–118, https://doi.org/10.1016/j.memsci.2010.11.055.
[46] M. Niederberger, Nonaqueous sol-gel routes to metal oxide nanoparticles, Acc. Chem. Res. 40 (2007) 793–800, https://doi.org/10.1021/ar600035e.
[47] C. Guizard, A. Ayral, M. Barboiu, A. Julbe, Sol–Gel processed membranes, in: L. Klein, M. Aparicio, A. Jitianu (Eds.), Handbook of Sol-Gel Science and Technology, Springer International Publishing, Cham, 2016, pp. 1–47, https://doi.org/10.1007/978-3-319-19454-7_58-1.
[48] J.E. Zhou, Q. Chang, Y. Wang, J. Wang, G. Meng, Separation of stable oil-water emulsion by the hydrophilic nano-sized ZrO2 modified Al2O3 microfiltration membrane, Sep. Purif. Technol. 75 (2010) 243–248, https://doi.org/10.1016/j.seppur.2010.08.008.
[49] J.-H. Eom, Y.-W. Kim, S.-H. Yun, I.-H. Song, Low-cost clay-based membranes for oily wastewater treatment, J. Ceram. Soc. Jpn. 122 (2014) 788–794, https://doi.org/10.2109/jcersj2.122.788.
[50] R. Cano-Crespo, B.M. Moshtaghioun, D. Gómez-García, R. Moreno, A. Domínguez-Rodríguez, Graphene or carbon nanofiber-reinforced zirconia composites: are they really worthwhile for structural applications? J. Eur. Ceram. Soc. 38 (2018) 3994–4002, https://doi.org/10.1016/j.jeurceramsoc.2018.04.045.
[51] R. Greenwood, K. Kendall, Selection of suitable dispersants for aqueous suspensions of zirconia and titania powders using acoustophoresis, J. Eur. Ceram. Soc. 19 (1999) 479–488, https://doi.org/10.1016/S0955-2219(98)00208-8.
[52] S.P. Rao, S.S. Tripathy, A.M. Raichur, Dispersion studies of sub-micron zirconia using Dolapix CE 64, Colloids Surf. A Physicochem. Eng. Asp. 302 (2007) 553–558, https://doi.org/10.1016/j.colsurfa.2007.03.034.
[53] C. Das, S. Bose, Advanced Ceramic Membranes and Applications, CRC Press, 2017.
[54] C. Li, W. Sun, Z. Lu, X. Ao, S. Li, Ceramic nanocomposite membranes and membrane fouling: a review, Water Res. 175 (2020), 115674, https://doi.org/10.1016/j.watres.2020.115674.
[55] F. Shojai, T. Mäntylä, Monoclinic zirconia microfiltration membranes: preparation and characterization, J. Porous Mater. 8 (2001) 129–142, https://doi.org/10.1023/A:1009694709010.
[56] H. Ranjan Sahu, G. Ranga Rao, Characterization of combustion synthesized zirconia powder by UV-vis, IR and other techniques, Bull. Mater. Sci. 23 (2000) 349–354, https://doi.org/10.1007/BF02708383.
[57] E. Eray, V. Boffa, M.K. Jørgensen, G. Magnacca, V.M. Candelario, Enhanced fabrication of silicon carbide membranes for wastewater treatment: from laboratory to industrial scale, J. Memb. Sci. (2020), 118080, https://doi.org/10.1016/j.memsci.2020.118080.
[58] T. Fengqiu, H. Xiaoxian, Z. Yufeng, G. Jingkun, Effect of dispersants on surface chemical properties of nano-zirconia suspensions, Ceram. Int. 26 (2000) 93–97, https://doi.org/10.1016/S0272-8842(99)00024-3.
[59] P. Boch, J.-C. Niepce, Ceramic Materials: Processes, Properties, and Applications, John Wiley & Sons, 2010.
[60] A. Pettersson, G. Marino, A. Pursiheimo, J.B. Rosenholm, Electrosteric stabilization of Al2O3, ZrO2, and 3Y–ZrO2 suspensions: effect of dissociation and type of polyelectrolyte, J. Colloid Interface Sci. 228 (2000) 73–81, https://doi.org/10.1006/jcis.2000.6939.
[61] B.A. Silva, V. De Souza, G. De Oliveira, M. Di Luccio, D. Hotza, K. Rezwan, M. Wilhelm, Characterization of functionalized zirconia membranes manufactured by aqueous tape casting, Ceram. Int. (2020), https://doi.org/10.1016/j.ceramint.2020.03.162.
[62] J. Cesarano, I.A. Aksay, A. Bleier, Stability of aqueous alpha-Al2O3 suspensions with poly(methacrylic acid) polyelectrolyte, J. Am. Ceram. Soc. 71 (1988) 250–255, https://doi.org/10.1111/j.1151-2916.1988.tb05855.x.
[63] X. Ding, Y. Fan, N. Xu, A new route for the fabrication of TiO2 ultrafiltration membranes with suspension derived from a wet chemical synthesis, J. Memb. Sci. 270 (2006) 179–186, https://doi.org/10.1016/j.memsci.2005.07.003.
[64] M.R.O, H. Mukhtar, Review on development of ceramic membrane from Sol-Gel route: parameters affecting characteristics of the membrane, IIUM Eng. J. 1 (2000) 1–6, https://doi.org/10.31436/iiumej.v1i2.334.
[65] X. Ju, P. Huang, N. Xu, J. Shi, Influences of sol and phase stability on the structure and performance of mesoporous zirconia membranes, J. Memb. Sci. 166 (2000) 41–50, https://doi.org/10.1016/S0376-7388(99)00243-4.
[66] F. Snijkers, A. de Wilde, S. Mullens, J. Luyten, Aqueous tape casting of yttria stabilised zirconia using natural product binder, J. Eur. Ceram. Soc. 24 (2004) 1107–1110, https://doi.org/10.1016/S0955-2219(03)00388-1.
[67] M.P. Albano, L.B. Garrido, K. Plucknett, L.A. Genova, Processing of porous yttria-stabilized zirconia tapes: influence of starch content and sintering temperature, Ceram. Int. 35 (2009) 1783–1791, https://doi.org/10.1016/j.ceramint.2008.10.003.
[68] R.V. Kumar, A.K. Ghoshal, G. Pugazhenthi, Fabrication of zirconia composite membrane by in-situ hydrothermal technique and its application in separation of methyl orange, Ecotoxicol. Environ. Saf. 121 (2015) 73–79, https://doi.org/10.1016/j.ecoenv.2015.05.006.
[69] Y.S. Lin, C.H. Chang, R. Gopalan, Improvement of thermal stability of porous nanostructured ceramic membranes, Ind. Eng. Chem. Res. 33 (1994) 860–870, https://doi.org/10.1021/ie00028a012.
[70] J. Etienne, A. Larbot, A. Julbe, C. Guizard, L. Cot, A microporous zirconia membrane prepared by the sol-gel process from zirconyl oxalate, J. Memb. Sci. 86 (1994) 95–102, https://doi.org/10.1016/0376-7388(93)E0141-6.
[71] S.D. Ramamurthi, Z. Xu, D.A. Payne, Nanometer-sized ZrOz particles prepared by a sol-emulsion-Gel method, J. Am. Ceram. Soc. 73 (1990) 2760–2763.
[72] K.B. Singh, M.S. Tirumkudulu, Cracking in drying colloidal films, Phys. Rev. Lett. 98 (2007), 218302, https://doi.org/10.1103/PhysRevLett.98.218302.
[73] M.S. Tirumkudulu, W.B. Russel, Cracking in drying latex films, Langmuir. 21 (2005) 4938–4948, https://doi.org/10.1021/la048298k.
[74] W.P. Yang, S.S. Shyu, E.-S. Lee, A.-C. Chao, Effects of poly(vinyl alcohol) content and calcination temperature on the characteristics of unsupported alumina membrane, Sep. Sci. Technol. 31 (1996) 1327–1343, https://doi.org/10.1080/01496399608006954.
[75] M. Copel, M. Gribelyuk, E. Gusev, Structure and stability of ultrathin zirconium oxide layers on Si(001), Appl. Phys. Lett. 76 (2000) 436–438, https://doi.org/10.1063/1.125779.
[76] J.P. Chang, Y.-S. Lin, S. Berger, A. Kepten, R. Bloom, S. Levy, Ultrathin zirconium oxide films as alternative gate dielectrics, J. Vac. Sci. Technol. B Microelectron. Nanometer Struct. 19 (2001) 2137, https://doi.org/10.1116/1.1415513.
[77] S. Ognier, C. Wisniewski, A. Grasmick, Characterisation and modelling of fouling in membrane bioreactors, Desalination 146 (2002) 141–147, https://doi.org/10.1016/S0011-9164(02)00508-8.
[78] C.N. Rani, S. Karthikeyan, S. Prince Arockia Doss, Photocatalytic ultrafiltration membrane reactors in water and wastewater treatment - a review, Chem. Eng. Process. Process. Intensif. 165 (2021), 108445, https://doi.org/10.1016/j.cep.2021.108445.
[79] J. Kaewsuk, G.T. Seo, Computational study of NF membrane removal in rejection of specific NOM compounds, Desalin. Water Treat. 51 (2013) 6218–6223, https://doi.org/10.1080/19443994.2013.780788.
[80] W. Balcerzak, J. Kwaśny, M. Kryłów, Oily wastewater treatment using a zirconia ceramic membrane : a literature review, Arch. Environ. Prot. 44 (2018) 3, https://doi.org/10.24425/122293.
[81] F. de Souza, S.R. Bragança, Extraction and characterization of humic acid from coal for the application as dispersant of ceramic powders, J. Mater. Res. Technol. 7 (2018) 254–260, https://doi.org/10.1016/j.jmrt.2017.08.008.
[82] G. Zhan, C. Li, D. Luo, Electrochemical investigation of bovine hemoglobin at an acetylene black paste electrode in the presence of sodium dodecyl sulfate, Bull. Korean Chem. Soc. 28 (2007) 1720–1724, https://doi.org/10.5012/bkcs.2007.28.10.1720.
[83] B. Braunschweig, W. Peukert, Protein Adsorption at the Electrified Air − Water Interface: Implications on Foam Stability, 2012.
[84] Y. Zhang, X. Shan, Z. Jin, Y. Wang, Synthesis of sulfated Y-doped zirconia particles and effect on properties of polysulfone membranes for treatment of wastewater containing oil, J. Hazard. Mater. 192 (2011) 559–567, https://doi.org/10.1016/j.jhazmat.2011.05.058.
[85] Q. Chang, J. Zhou, Y. Wang, J. Wang, G. Meng, Hydrophilic modification of Al2O3 microfiltration membrane with nano-sized γ-Al2O3 coating, Desalination 262 (2010) 110–114, https://doi.org/10.1016/j.desal.2010.05.055.
[86] F. Shojai, T.A. Mäntylä, Structural stability of yttria doped zirconia membranes in acid and basic aqueous solutions, J. Eur. Ceram. Soc. 21 (2001) 37–44, https://doi.org/10.1016/S0955-2219(00)00163-1.
[87] M.L. Tummino, E. Laurenti, F. Deganello, A. Bianco Prevot, G. Magnacca, Revisiting the catalytic activity of a doped SrFeO3 for water pollutants removal: effect of light and temperature, Appl. Catal. B 207 (2017) 174–181, https://doi.org/10.1016/j.apcatb.2017.02.007.

Glossary

Al_2O_3: alumina
COD: chemical oxygen demand (mg L^{-1})
DM: duramax™ D-3005
DP: dolapix CE 64

DLS: dynamic light scattering
EDS: energy dispersive X-ray spectroscopy
MF: microfiltration
MW: molecular weight
NF: nanofiltration
CS 76: optapix CS 76
PAF 2: optapix PAF 2
LMH/bar: permeability (L m^{-2} h^{-1} bar^{-1})
SEM: scanning electron microscopy
SiO_2: silica
SiC: silicon carbide
TOC: total organic carbon (mg L^{-1})
TMP: transmembrane pressure (bar)
UF: ultrafiltration
XRD: X-ray diffraction
YSZ: yttria-stabilized zirconia
Z-1: zirconia powder -1 μm
Z-2: zirconia powder -2 μm
ZrO_2: zirconia